Evaluation of Corrosion Rates of Reinforcing Bars for Probabilistic Assessment of Existing Road Bridge Girders

Payal K. Firodiya[1]; Amlan K. Sengupta, P.E.[2]; and Radhakrishna G. Pillai[3]

Abstract: The rate of corrosion of the reinforcing bars is one of the important parameters required to estimate the residual service-life of a reinforced concrete (RC) bridge deck. In the present study, first, the linear polarization resistance technique was used to measure the corrosion rates of plain mild steel and cold twisted deformed (CTD) bar specimens, which were typically used in the older existing bridges. To consider the variability of a corrosion rate, the frequency distributions of the corrosion rates for the two types of bars were determined. Next, a probabilistic approach was adopted for assessing an existing RC girder-and-slab road bridge deck, subjected to corrosion of bars attributable to air-borne chlorides. A computational model was developed using the Monte Carlo simulation method, to assess the reduction in the flexural capacity of a typical girder. It was observed that the reduction in the mean capacity and the dispersion of the capacity with respect to time, were high with the measured statistical parameters of the corrosion rate of CTD bars. **DOI: 10.1061/(ASCE)CF.1943-5509.0000579.** © *2014 American Society of Civil Engineers.*

Author keywords: Corrosion rate; Cold twisted deformed bars; Flexural capacity; Linear polarization resistance; Reinforcing bar; Reinforced concrete bridge girder.

Introduction

Plain mild steel (MS) and cold twisted deformed (CTD) steel reinforcing bars were used in the construction of reinforced concrete (RC) bridges in India until a few decades ago. With the introduction of high strength CTD bars with surface ribs during the late 1960s, the required amount of steel in an RC structure declined. Hence, CTD bars became popular in the construction of RC structures including bridges. However, the reduced ductility and higher corrosion potential of CTD bars were realized subsequently. There are several RC bridges in the coastal and marine environments, which have shown distress owing to the ingress of moisture and chloride ions. In the presence of oxygen and water, corrosion of steel bars is initiated. Because of corrosion, there is reduction in the cross-sectional area of the bars, and formation of rust. It leads to cracking and spalling of the concrete cover surrounding the rusted bars. This affects the long-term serviceability and strength of the structural system. To avoid unexpected and sudden failure, service-life estimation, performance monitoring and maintenance of the bridges have become essential.

The deterioration process depends on many factors, e.g., the quality of concrete, concrete cover for the bars, the concentration of chloride ions in the ambient environment, temperature and humidity conditions, and the rate of corrosion (or, corrosion rate) for the bars. The corrosion rate is one of the important parameters required to estimate the residual cross-sectional area of the bars, which in turn is necessary for predicting the residual service-life

of a bridge. It is influenced by the type of steel and the manufacturing process for the bars. In the present study, an experimental program was undertaken to determine the corrosion rates of MS and CTD bars, so that appropriate values are used in the analysis of existing bridges.

The deterioration of RC bridge decks can be studied based on a deterministic approach. However, a deterministic method may have a large margin of error in predicting the service life, because the factors affecting corrosion have many uncertainties. It is more appropriate to adopt a probabilistic approach to model the deterioration of flexural capacity with time attributable to corrosion of bars. The use of experimentally evaluated statistical parameters for the corrosion rates of MS and CTD bars would give a more realistic prediction for the existing bridges made of such bars. However, the required information for the corrosion rates of the two types of bars, based on significant number of specimens from India, could not be found in the literature. Hence, in the present study, the aim was to test large number of specimens for the MS and CTD bars under similar exposure conditions and procedures, and derive the frequency distributions for the corrosion rates. The results were used to model the deterioration of flexural capacity of the girders of a typical existing girder-and-slab bridge deck, using a probabilistic approach.

Research Significance

Many old/existing reinforced concrete bridges are experiencing corrosion. The quantification of the variability of corrosion rates of reinforcing bars (rebar) is important in probabilistic prediction of the residual or remaining service life of reinforced concrete bridges subjected to corrosion of the bars. The statistical estimates of the corrosion rates of one type of rebar (say, MS) can be different from that of another type (say, CTD) owing to the variations in the chemical compositions and manufacturing processes. The quantitative information on corrosion rates available in the reviewed literature is mostly limited to the types of bars used in a specific country, with restricted statistical parameters. The present study

[1]Engineer, G A Bhilare Consultants Pvt. Ltd., Pune 411004, India.
[2]Associate Professor, Dept. of Civil Engineering, Indian Institute of Technology Madras, Chennai 600036, India (corresponding author). E-mail: amlan@iitm.ac.in
[3]Assistant Professor, Dept. of Civil Engineering, Indian Institute of Technology Madras, Chennai 600036, India.

determined the corrosion rates of MS and CTD bars which were typically used in existing bridges, and demonstrated their use in a probabilistic assessment of the deterioration of flexural capacity of a selected bridge deck/girder system.

Background Information

Modeling of Corrosion of Reinforcing Bars

The chloride-ion induced corrosion of steel reinforcing bars can be modelled as a two-stage process. The *corrosion initiation phase* is the time from the construction of the structure to the time when the amount of permeated chloride ions exceeds a certain threshold value to breakdown the passive layer of ferrous oxides on the surface of a bar. The permeation of chloride ions is modelled by the Fick's second law of diffusion. The corrosion initiation time in years (t_0) can be obtained by an approximate solution to the Fick's law as follows (IRC 2002):

$$t_0 = \frac{C_0 c^2}{12 D_C (\sqrt{C_0} - \sqrt{C_{th}})^2} \tag{1}$$

Here, C_0 = equilibrium chloride concentration (kg/m^3) on the exposed surface of concrete, C_{th} = threshold value of chloride concentration (kg/m^3), c = concrete cover thickness (mm), and D_C = coefficient of chloride diffusion through concrete (mm^2/year). However, there are uncertainties in all these variables, thus affecting the initiation time.

After initiation of corrosion, there is reduction in the net section of a bar. Although chloride-ion induced corrosion causes pitting on the surface of a bar, the pitting is randomly distributed on the surface in absence of major cracks or in the presence of distributed cracks of small width. A uniform reduction in the diameter of the bar can be assumed for modelling the reduction in the net section. The total cross-sectional area of the bars in a layer (A_{st}) is given as a function of time (t) as follows:

$$A_{st} = \begin{cases} \dfrac{n\pi}{4} \varphi^2, & t \leq t_0 \\ \dfrac{n\pi}{4} [\varphi - 2r(t - t_0)]^2, & t > t_0 \end{cases} \tag{2}$$

Here, n = number of bars in a layer; φ = initial nominal diameter of a bar, and r = corrosion rate for the bars in uncracked concrete. The time required for showing initial distress attributable to formation of rust, cracking and staining of the concrete cover is termed as the *corrosion propagation phase*. Liu and Weyers (1998) modelled the time to first cracking as a function of the strength and thickness of concrete cover, and the corrosion rate of bars. A simplified model for estimating the time to first cracking beyond t_0 is given as $t_{cr} = 80c/\varphi r$, where t_{cr} is in years, c is the thickness of the cover in mm, φ is in mm and r is in mm/year (IRC 2002).

The time for severe cracking and spalling of concrete cover is the propagation time (t_1), whose value can be estimated as $t_1 = t_0 + 10 t_{cr}$ (Val and Stewart 2003). Beyond this, the corrosion rate of bars increases because of contact with the atmosphere. If the previous model of stable corrosion is extended, the total area of the net section of the bars in a layer (A_{st}) as a function of time ($t > t_1$) is given as follows. Here, r_1 = increased corrosion rate of bars, after being exposed to atmosphere

$$A_{st} = \frac{n\pi}{4} \{\varphi - 2[r(t_1 - t_0) + r_1(t - t_1)]\}^2 \tag{3}$$

Literature Review

Measurement of Corrosion Rates

In an experimental program, to determine the corrosion rate of bars embedded in concrete or mortar, the initiation of corrosion can be accelerated in several ways: Application of electrical potential, cyclic wetting and drying in salt solution, adding chlorides to the concrete, and spraying salt solution at regular intervals in a salt spray chamber (Castro et al. 1997). Next, to determine the corrosion rate, many measurement techniques have been used, such as macrocell corrosion test, half-cell potential technique, gravimetric mass loss method, AC impedance spectroscopy, and linear polarization resistance technique. The convenience of the linear polarization resistance (LPR) technique is that, a small potential shift produces a measurable amount of current (Tait 1994). Based on LPR tests of slab specimens, the corrosion rates of CTD bars were found to be higher than thermomechanically treated (TMT) bars (Pradhan and Bhattacharjee 2009). The corrosion rates in the specimens using ordinary portland cement were found to be the highest, as compared with those from specimens using portland slag cement and portland pozzolana cement.

Service-Life Estimation of Bridges

The assessment of bridge decks based on the probabilistic approach is briefly presented. Frangopol et al. (1997) presented a method to analyze the reliability of RC bridge girders subjected to corrosion. The solution was based on a nonlinear optimization software and Monte Carlo simulation technique. Parametric studies were performed by varying the values of mean and coefficient-of-variation of the variables related to corrosion (Enright and Frangopol 1998). The loss of the flexural capacity of a bridge girder attributable to corrosion, was formulated in terms of a resistance loss function.

A time-dependent reliability analysis of bridge decks was demonstrated by Stewart and Rosowsky (1998). Klinghoffer et al. (2000) demonstrated a method of estimating the service life of an RC member based on the reduction of the area of the reinforcing bars. Assessment of performance of an RC member using time-dependent reliability method was proposed by Li and Melchers (2005). Pillai et al. (2010) proposed a framework to determine the reliability index for a posttensioned segmental bridge deck, based on the Monte Carlo simulation.

Experimental Evaluation of Corrosion Rates

In the present study, the LPR technique was adopted to measure the corrosion rates of MS and CTD bar specimens, at controlled room temperature of 25°C and 60% relative humidity. Because the above types of bars are not readily available in the market, specimens of bars of 16-mm diameter were collected from stocks in the laboratory. A total of 50 test specimens for each of the two types of bars were prepared. A spindle shaped specimen was prepared by embedding a cut-piece of a bar in a mortar cylinder of diameter 40 mm (Fig. 1). A low uniform thickness of cover of 12 mm was used to reduce the corrosion initiation time. For improved homogeneity with respect to diffusion of chlorides, and ease of casting, cement mortar was selected instead of concrete.

Because the bars were old, there were patches of rust on the bars, especially the CTD bars. First, the bar pieces were cleaned
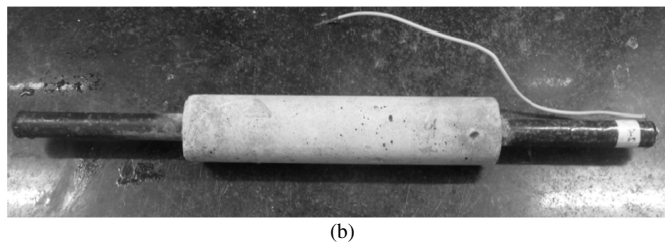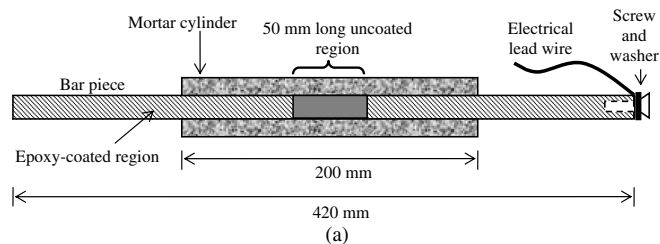
Fig. 1. Test specimen: (a) schematic diagram; (b) a typical specimen

to remove the rust as per the procedure given in ASTM (2011). A bar piece was dipped in a solution of hydrochloric acid, hexamethylene tetramine and reagent water for 10 min. After soaking in fresh water, the piece was dipped in diluted acetone solution and cleaned with a wire brush. The MS bars were relatively rust-free; therefore, they were cleaned only with diluted acetone solution.

Next, a bar piece was internally threaded at one end to fit a screw with an electrical lead wire for connecting to the potentiostat. The screw was of 6-mm diameter and 10-mm length. A copper wire was wound around the screw and tightened with a washer. After inserting the screw into the threaded end, the bar piece was coated with two-part epoxy (resin and hardener), leaving the central 50-mm region exposed. This was done to ensure that only the central 50-mm region of the bar was exposed to corrosion. The screw and washer were also coated with epoxy. A total of three epoxy coats were
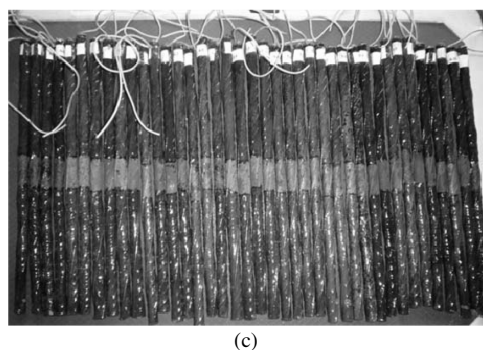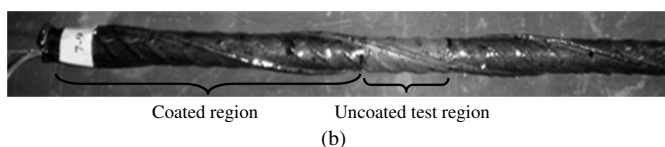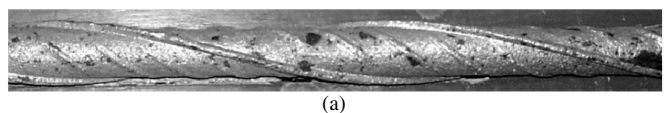
applied to the piece. After application of one coat, the bar was allowed to dry for 24 h and then the next coat was applied. A few photographs of stages of preparation of specimens are shown in Fig. 2.

The mold for casting mortar was prepared from a piece of PVC pipe. A slit was provided along the length of the pipe for ease of demolding. To cast a specimen vertically, a cap was provided at the bottom. The bar piece was placed through a hole in the cap. The mortar for all the 50 specimens of a type of bar was cast at a time. For the mortar, a water:cement:sand ratio of 0.55:1.0:2.75 by weight was selected, without any admixture. Ordinary portland cement and standard grade of sand were used, as was common in the construction of old bridges. After casting, another cap was placed at the top to maintain the bar piece centrally. The molds were removed after 23 ± 1 h. After this, the specimens were cured in saturated lime water.

Corrosion Tests

The cured specimens were subjected to alternate wetting and drying to accelerate the initiation of corrosion. The specimens were immersed in 3.5% sodium chloride (NaCl) solution for a period of seven days. The submerged condition was considered to be the wet exposure condition. Next, the specimens were allowed to air dry in a container for seven days. This was considered to be the dry exposure condition. At the end of each wetting and drying period, LPR test readings were taken for the specimens to measure the corrosion rates. The alternate wetting and drying cycles were continued for a period of 56 days. By this time, the mortar had almost hydrated. The first two sets of readings up to 14 days were neglected in the subsequent computations to avoid initial noise in the data collected.

The LPR test was conducted using a three-electrode corrosion cell setup (Fig. 3). The corrosion cell consisted of a specimen, a counter electrode, a reference electrode and 3.5% NaCl electrolytic

Fig. 2. Preparation of test specimens: (a) after cleaning; (b) after epoxy-coating; (c) a set of bars before casting
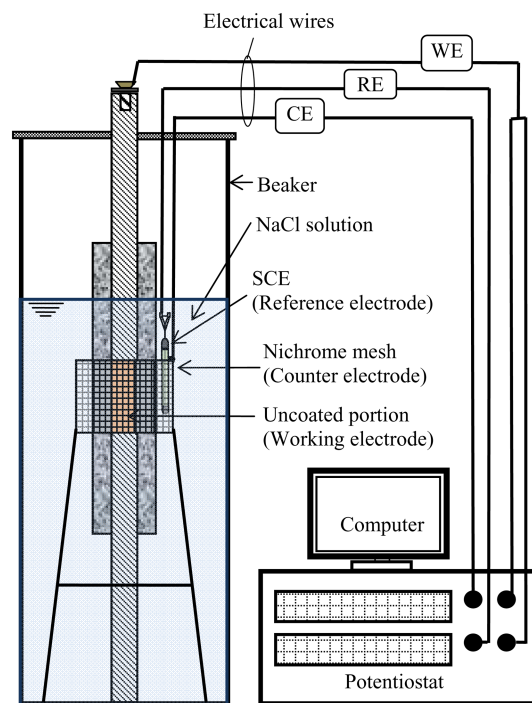
Fig. 3. Schematic diagram of setup for linear polarization resistance test
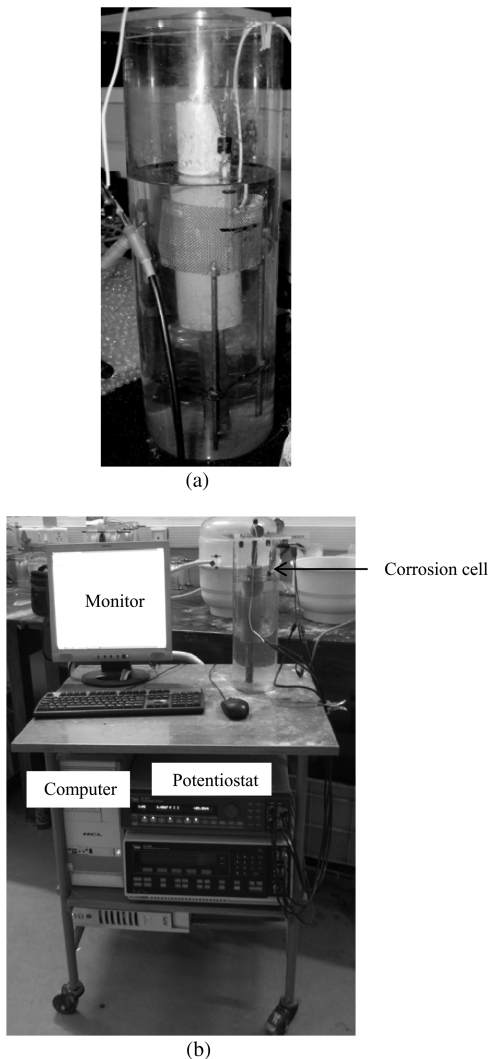
Fig. 4. Setup for linear polarization resistance test: (a) corrosion cell; (b) workstation

solution placed in a glass container. The central 50-mm uncoated region of the bar in the specimen was the working electrode (WE). A cylindrical Nichrome mesh of 64-mm diameter was used as the counter electrode (CE). A saturated calomel electrode (SCE) was used as the reference electrode (RE). It was positioned such that its tip remained in close proximity with the working electrode. The lead wires from the electrodes were connected to the Solartron 1287 potentiostat. A computer recorded the data from the LPR tests. The workstation for the tests is shown in Fig. 4.

When the current through a specimen (WE) is zero, the electrical potential of the specimen is termed as the open circuit potential (OCP). The OCP of the WE was measured prior to each LPR test reading. After measuring the OCP, an external potential was applied to the WE. The range of polarization was ±15 mV with respect to the measured OCP. The generated electrical current through the electrode was measured using the potentiostat. The current (I) was plotted with respect to the applied potential (E) to generate the polarization curve. The slope of the polarization curve at zero current and the Stern-Geary constant equal to 26 mV were used to calculate the corrosion current density (i_{corr}) using the *CORRWARE* software. The corrosion current density was converted to the corrosion rate of a plate (h_{corr}) in millimetres loss per year (mm/year) using the following equation (Tait 1994):
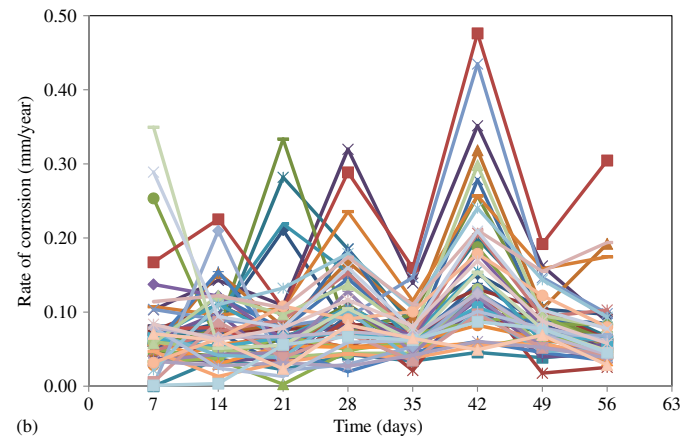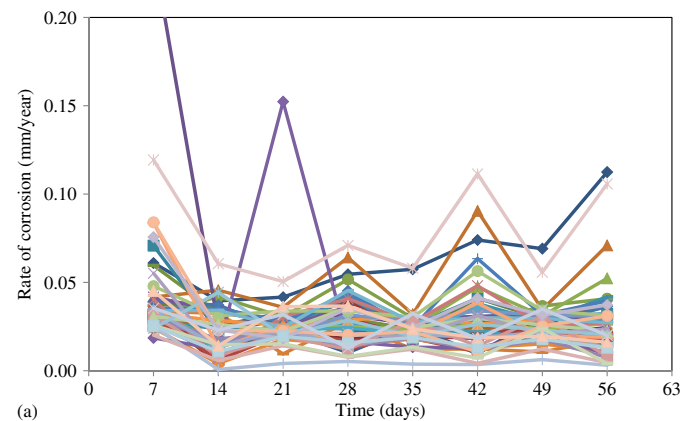
Fig. 5. Rates of corrosion obtained from LPR tests for: (a) MS bars; (b) CTD bars

$$h_{corr} = \frac{i_{corr} Z E_Q}{\rho_{st}} \qquad (4)$$

Here, constant $Z = 128,660$, equivalent weight of steel $E_Q = 27.92$ g, and density of steel $\rho_{st} = 7.6$ g/cm³. To obtain the instantaneous rate of corrosion of the bar in terms of loss of radius per year (in mm/year), a conversion factor was calculated based on equivalent mass loss as per Faraday's law (Firodiya 2013).

Test Results

The instantaneous corrosion rates of the specimens (r) at the end of each of wet and dry exposure conditions were measured (Fig. 5). Because there was a fluctuating trend in the values for the two conditions, they were grouped separately. Here, r_w and r_d denote the corrosion rates after the wet and dry conditions, respectively. There were wide variations in the corrosion rates among the specimens. However, for each of r_w and r_d, there was no detectable pattern of variation with respect to time.

Assuming that a corrosion rate is independent of time, a histogram was plotted for all the values from 50 specimens after each of the two exposure conditions. Also, the values of mean and standard deviation were obtained. The appropriate frequency distribution was determined from several theoretical probability distribution functions, by the Kolmogorov-Smirnov (K-S) goodness-of-fit test. In the K-S test, the cumulative frequency distribution obtained from the test results was compared with that of the trial distribution function. It was observed that the lognormal distribution was suitable for both the dry and wet conditions of MS and CTD bars. The histogram plots for the corrosion rates along with the distribution
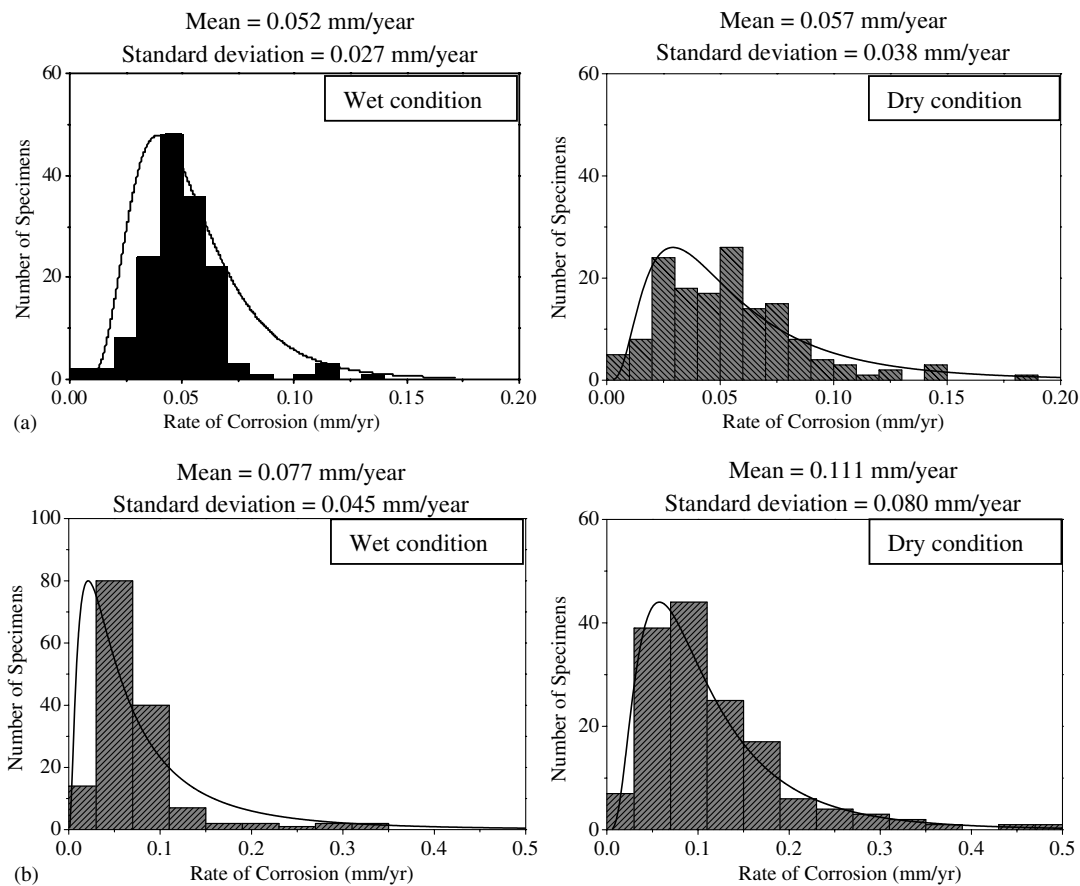
Fig. 6. Histograms and frequency distribution diagrams for measured corrosion rates for: (a) MS bars; (b) CTD bars

functions, are shown in Fig. 6. The mean values of the corrosion rates for the 50 specimens of each of MS and CTD bars, are presented in Table 1.

It can be observed that the average corrosion rate of MS bars under dry exposure is 10% higher than that in the wet (submerged) condition. However, the average corrosion rate of CTD bars under dry exposure is almost 50% higher than that in wet condition. The higher corrosion rate under dry exposure may be attributed to availability of oxygen and moisture in the mortar cylinder. For either type of bars, the dispersion in the corrosion rate is significantly higher in the dry condition.

Next, it is observed that the corrosion rate of CTD bars in wet condition is 1.4 times greater than that of MS bars. In dry condition,

the corrosion rate of CTD bars is almost two times greater than that of MS bars. The increase in corrosion rate for CTD bars is primarily attributable to the cold twisting process, which generates the well-known residual stresses (Callister 2003). Also, the higher increase in corrosion rate in dry condition is expected to be due to the partial saturation condition, as compared with the wet condition with complete saturation. The uneven surface and spiral ribs that can trap moisture and oxygen, might have also played a role in increasing the corrosion activities.

Numerical Assessment of Bridge Girders

In the present study, a typical RC girder-and-slab road bridge deck constructed in a coastal area was selected. The data for the deck was obtained from the as-built design drawings (Fig. 7). In the present study, a typical girder was selected for assessment of the longitudinal flexural capacity. The sectional and pertinent reinforcement details for a girder are shown in Fig. 8. The longitudinal flexural reinforcement was of CTD bars of design yield strength equal to 415 MPa. The design cube compressive strength of concrete was 30 MPa.

Reduction in Flexural Capacity

For the given section of the girder, the neutral axis at the ultimate state lies within the depth of the flange. Hence, the section can be assumed to behave as a rectangular section. The flexural capacity for a rectangular section (M_{uR}), is given by the following equation:

Table 1. Measured Corrosion Rates

Test time (days)	Exposure condition	Average corrosion rates (mm/year)	
		MS bars	CTD bars
21	Wet	0.055	0.082
28	Dry	0.056	0.111
35	Wet	0.048	0.07
42	Dry	0.06	0.157
49	Wet	0.054	0.085
56	Dry	0.054	0.072
Overall mean	Wet	0.052	0.077
	Dry	0.057	0.111
Standard deviation	Wet	0.027	0.045
	Dry	0.038	0.080
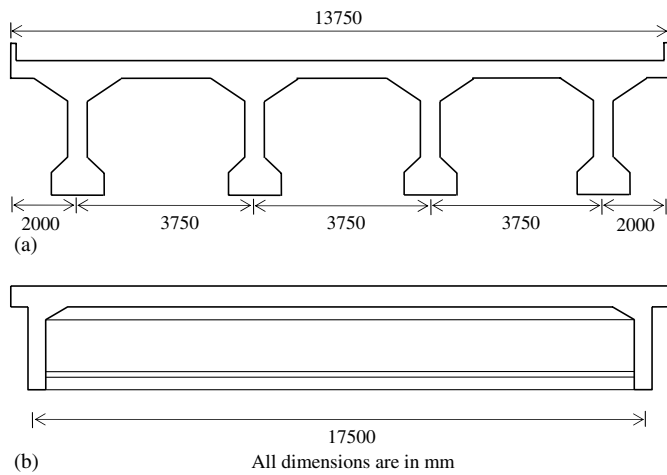
Fig. 7. Sectional details of the bridge deck: (a) cross section; (b) longitudinal section
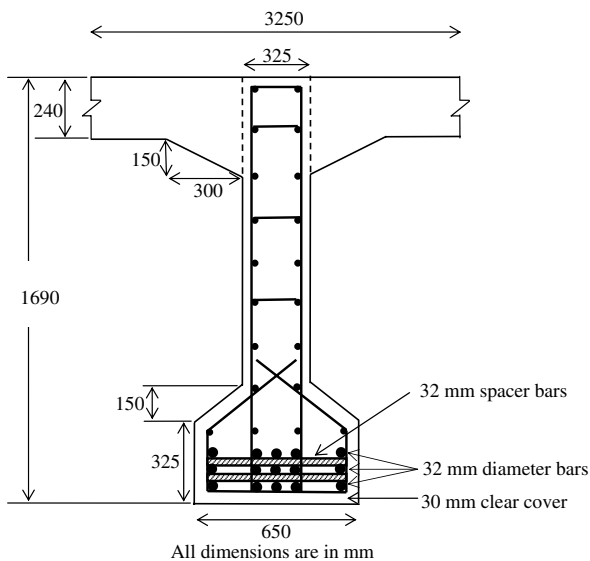
Fig. 8. Sectional and pertinent reinforcement details at mid-span of girder

$$M_{uR} = f_s A_s \left(1 - k_2 \frac{f_s A_s}{k_1 k_3 f_c b_f d} \right) d \qquad (5)$$

Here, A_s = area of the longitudinal tensile reinforcement, f_s = yield strength of the steel, d = effective depth of the reinforcement, f_c = compressive strength of concrete, and b_f = width of the flange. The value of k_1 (conversion factor for compressive stress block of

concrete) for a parabolic-rectangular stress block is 0.81. The value of k_2 (ratio of the depth of centroid of the stress block to the depth of neutral axis) for a parabolic-rectangular stress block is 0.42. The value of k_3 (ratio of the compressive strength of concrete in the girder to that of the design cube compressive strength of concrete) was taken as 0.67, which is based on the size factor equal to 0.85 while using cylinder compressive strength, and the conversion of cylinder strength to cube strength (Pillai and Menon 2009). Any material safety factor or strength reduction factor were not considered in the analysis. As per the section details, before the initiation of corrosion, $A_s = A_{s0} = 12{,}064$ mm^2, and the corresponding flexural capacity is denoted as M_{uR0}.

In the probabilistic assessment of the bridge deck, in addition to the variables related to corrosion, the strengths of the materials were considered to be random variables to account for the uncertainties in manufacturing and casting. The distributions and statistical parameters of the random variables considered in the analysis are given in Table 2. Because the girders are predominantly under dry condition with occasional wetting during rains, the parameters for the corrosion rate of CTD bars in dry condition, as obtained from the experimental program were used. The rest of the parameters were suitably selected from the literature.

The distribution of the flexural capacity of the girder at a certain time (t) was calculated by Monte Carlo simulation in a computational model using MATLAB, with number of simulations $N = 100{,}000$. For each set of the random variables, the corrosion initiation time was calculated using Eq. (1). Once the corrosion has initiated, the deterioration in the capacity of the girder is only attributable to reduction in the cross-sectional area of the bottom row of bars, assuming that the distributions of strength of steel and concrete do not change with time. At time t, the net area of the bars ($A_s = A_{st}$) was determined using Eqs. (2) or (3), and the flexural capacity ($M_{uR} = M_{uRt}$) was estimated using Eq. (5). The slight change in d with time was neglected. The N values of flexural capacities were calculated using the N sets of random realizations of each random variable considered. For each time step, the statistical parameters [mean $E(M_{uRt})$ and standard deviation σ_t] of the distribution of the flexural capacity were calculated. An abridged version of the algorithm for the simulation is given in Fig. 9. The process was repeated for different values of time until the mean of time to severe cracking [$E(t_1)$]. Beyond $E[t_1]$, in absence of values for r_1, the calculation was continued for demonstration, by extrapolating the parameters for r. However, after severe cracking, r_1 is expected to be higher than that estimated from the specimens with uncracked mortar.

The variation of $E[M_{uRt}]$ with time is shown in Fig. 10. Beyond $t = E[t_1]$, the trend is shown by a dashed line. It can be observed that the mean flexural capacity decreases by 4% at 17.5 years [$t = E(t_1)$] and by 18% at 50 years, after the construction of the bridge. The high corrosion rate of the CTD bars influences the decay in the flexural capacity. The variations of $E[M_{uRt}] \pm 1.65\sigma_t$ for the

Table 2. Statistical Parameters of Selected Random Variables

Random variable	Selected distribution	Mean	Standard deviation	Units	Source
Concrete cover depth (c)	Normal	30.0	9.5	mm	Weyers (1998)
Surface chloride concentration (C_0)	Lognormal	2.95	1.48	kg/m^3	Vu and Stewart (2000)
Threshold chloride concentration (C_{th})	Uniform	0.9	0.17	kg/m^3	Vu and Stewart (2000)
Chloride diffusion coefficient (D_C)	Lognormal	63.1	47.3	mm^2/year	Vu and Stewart (2000)
Rate of corrosion for CTD bars (r)	Lognormal	0.111	0.08	mm/year	LPR tests
Compressive strength of concrete (f_c)	Normal	37.5	5.63	N/mm^2	Ranganathan (1999)
Yield strength of steel (f_s)	Normal	468.0	46.89	N/mm^2	Ranganathan (1999)

© ASCE

J. Perform. Constr. Facil.
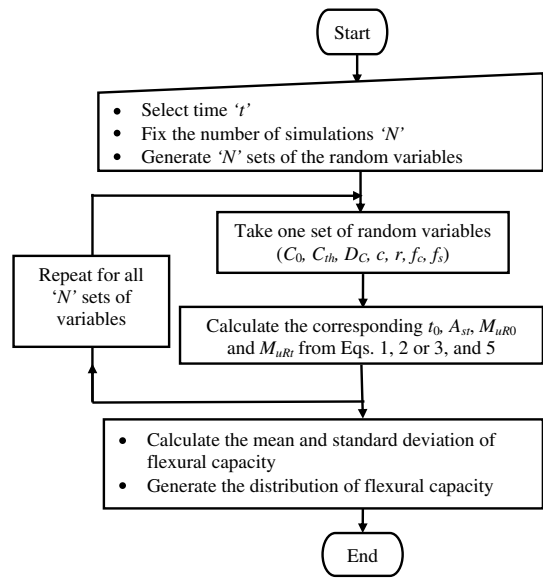
Fig. 9. Algorithm for Monte Carlo simulation (abridged)
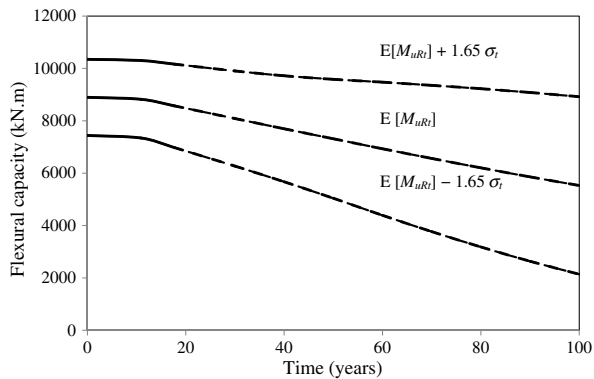
Fig. 10. Time-variant flexural capacity of the girder

flexural capacity are also plotted to show the dispersion, corresponding to approximately 5 and 95 percentile estimates, assuming a normal distribution for M_{uRt}. It is observed that with the increase in the standard deviation of the flexural capacity with time, the dispersion gets wider. The coefficient of variation of the flexural capacity changes from 0.11 at 17.5 years to 0.19 at 50 years. This reflects increased probability of failure of the girder with time.

Effects of Design Variables

The effects of initial selection of mean cover thickness and bar size (the total area of steel being constant) on the time-variant flexural capacity of the girder was studied. The flexural capacity was computed for four values of bar diameter (16, 20, 25, and 32 mm) and four values of mean cover thicknesses (30, 40, 50, and 60 mm). The value of d was kept same. Figs. 11(a and b) show the time-variant flexural capacities up to 50 years for different bar sizes and cover thicknesses, respectively. From Fig. 11(a) it is observed that the reduction in $E[M_{uRt}]$ is more for smaller size bars. Hence, larger bar size is preferred to reduce the effect of corrosion. However, if the girder cracks under service loads, the bar size should be restricted to limit the flexural crack width. From Fig. 11(b) it is observed that reduction in $E[M_{uRt}]$ is more for lower cover thickness.
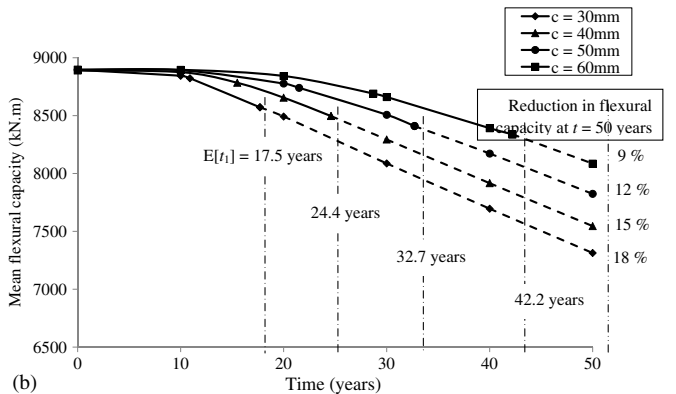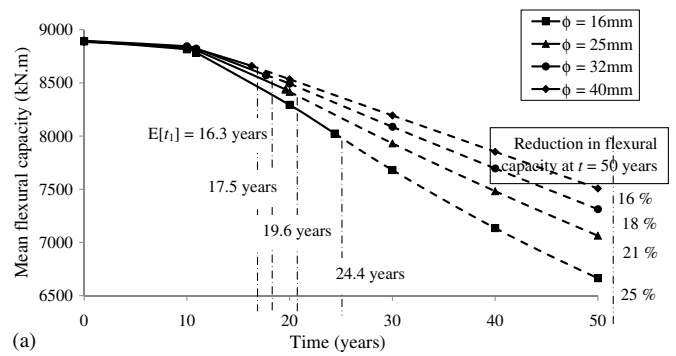
Fig. 11. Effect of design variables on the time-variant flexural capacity of the girder for: (a) different bar sizes ($c = 30$ mm); (b) different cover thicknesses ($\varphi = 32$ mm)

Table 3. Normalized Variables and Their Parameters

Normalized variable	Symbol and expression	Mean	Coefficient of variation (COV)	Distribution
Compressive strength of concrete (Y_1)	$Y_1 = \frac{f_c}{f_{ck}}$	1.246	0.15	Normal
Yield strength of steel (Y_2)	$Y_2 = \frac{f_s}{f_y}$	1.125	0.10	Normal
Cross-sectional area of bars (Y_3)	$Y_3 = \frac{A_{st}}{A_{s0}}$	As obtained from the simulation		
Depth of neutral axis (Y_4)	$Y_4 = \frac{x_{ut}}{x_{u0}}$	As obtained from the simulation		

Hence, higher cover thickness is required to reduce the effect of corrosion. The highest value of cover thickness was restricted to 60 mm, so that if the girder cracks under service loads, the flexural crack width is limited.

Normalization of Variables

In another computational model, the random variables were normalized to make the procedure generic for similar bridge girders. The normalized variables and their statistical parameters are given in Table 3. Here, x_{ut} is the time-variant depth of the neutral axis and x_{u0} is the depth before the initiation of corrosion. The ratio of the instantaneous flexural capacity of a bridge girder to the initial flexural capacity was defined as the normalized flexural capacity (M_{uRt}/M_{uR0}). Substituting the normalized variables from Table 3, the normalized flexural capacity of the girder is given as follows:

© ASCE   04014067-7   J. Perform. Constr. Facil.
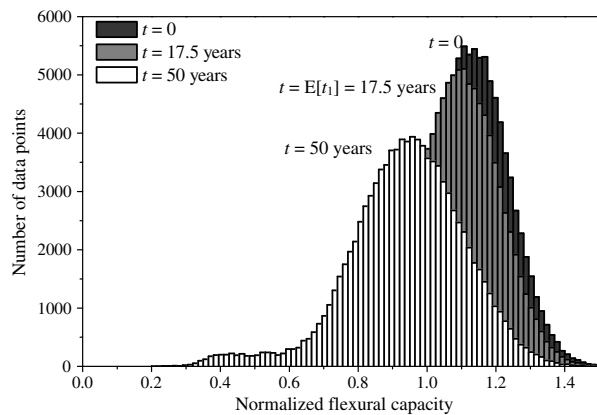
Fig. 12. Variation of distribution of normalized flexural capacity of a girder

$$\frac{M_{uRt}}{M_{uR0}} = \frac{Y_1 Y_4 \left(\frac{d}{x_{u0}} - k_2 Y_4\right)}{\left(\frac{d}{x_{u0}} - k_2\right)} \tag{6}$$

The values of mean $[E(M_{uRt}/M_{uR0})]$, standard deviation and distribution of the time-variant normalized flexural capacity were calculated for a set of standard girder sections with increasing depth, but the same amount of longitudinal reinforcement. The variation in distribution of the normalized flexural capacity of the section in Fig. 8, with respect to time, is shown in Fig. 12. With the experimentally measured statistical parameters of the corrosion rate, the reduction in the mean of the normalized flexural capacity and the increase of the spread in the distribution, for the selected set of girder sections were similar.

Conclusions

The observations and conclusions from the present study are as follows:
1. The statistical parameters and distributions for the rates of corrosion for MS and CTD bars were determined experimentally. The mean corrosion rates of the MS bars under wet and dry exposure conditions were 0.052 and 0.057 mm/year, respectively. The corresponding values for the CTD bars were 0.077 and 0.111 mm/year, respectively. The high corrosion rates for the CTD bars can be attributed to the residual stresses generated during the cold twisting process. A lognormal distribution was found to be suitable to model the variability of a corrosion rate.
2. A typical girder of a girder-and-slab road bridge deck was assessed for the reduction in flexural capacity with time, attributable to chloride-ion induced corrosion of the steel reinforcing bars. Monte Carlo simulation was adopted to determine the distribution of the flexural capacity of a girder at a certain time after the construction of the bridge, based on the experimentally determined distribution of the corrosion rate of CTD bars, for dry exposure condition. It was observed that the mean flexural capacity decreases by 18% at 50 years, after the construction of the bridge. Also, the dispersion of the flexural capacity gets larger with time.
3. The effects of variations in cover thickness and bar size on the time-variant flexural capacity of the girder were studied. It was observed that at 50 years, the reductions in mean flexural capacity were 25, 21, 18, and 16% for bar diameters of 16, 25, 32, and 40 mm, respectively. Also, the reduction in mean

flexural capacity was 18, 15, 12, and 9% for cover thicknesses of 30, 40, 50, and 60 mm, respectively. These values provide quantitative information on the detrimental effect of using smaller bars and reduced cover in a bridge girder subjected to chloride-ion induced corrosion.
4. The use of normalized random variables for the generic assessment of flexural capacity of similar bridge girders was demonstrated. It was observed that if the statistical parameters of the corrosion rates were the same, the reduction in the mean of the normalized flexural capacity and the increase of the spread in the distribution, for the selected set of sections were similar.

Acknowledgments

References

ASTM. (2011). "Standard test method for determining effects of chemical admixtures on corrosion of embedded steel reinforcement in concrete exposed to chloride environments." *G1–03*, West Conshohocken, PA.

Callister, W. J. (2003). *Materials science and engineering—An introduction*, 6th Ed., Wiley, Hoboken, NJ.

Castro, P., Veleva, L., and Balancan, M. (1997). "Corrosion of reinforced concrete in a tropical marine environment and in accelerated tests." *Constr. Build. Mater.*, 11(2), 75–81.

CORRWARE [Computer software]. Southern Pines, NC, Scribner Associates.

Enright, M. P., and Frangopol, D. M. (1998). "Probabilistic analysis of resistance degradation of reinforced concrete bridge beams under corrosion." *Eng. Struct.*, 20(11), 960–971.

Firodiya, P. (2013). "Evaluation of corrosion rates of reinforcing bars and assessment of deterioration of flexural capacity of road bridge girders." M.S. thesis, Indian Institute of Technology Madras, Chennai, India.

Frangopol, D. M., Lin, K.-Y., and Estes, A. C. (1997). "Reliability of reinforced concrete girders under corrosion attack." *J. Struct. Eng.*, 10.1061/(ASCE)0733-9445(1997)123:3(286), 286–297.

Indian Roads Congress (IRC). (2002). "An approach document for assessment of remaining life of concrete bridges." *IRP:SP–60–2002*, New Delhi, India.

Klinghoffer, O., Frølund, F., and Poulsen, E. (2000). "Rebar corrosion rate measurements for service life estimates." *The fall convention*, American Concrete Institute, Toronto, ON.

Li, C. Q., and Melchers, R. E. (2005). "Time-dependent risk assessment of structural deterioration caused by reinforcement corrosion." *ACI Struct. J.*, 102(5), 754–762.

Liu, Y., and Weyers, R. E. (1998). "Modeling the time-to-corrosion cracking in chloride contaminated reinforced concrete structures." *ACI Mater. J.*, 95(6), 675–681.

MATLAB [Computer software]. Natick, MA, MathWorks.

Pillai, R. G., Hueste, M. D., Gardoni, P., Trejo, D., and Reinschmidt, K. F. (2010). "Time-variant service reliability of post-tensioned segmental concrete bridges exposed to corrosive environments." *Eng. Struct.*, 32(9), 2596–2605.

Pillai, S. U., and Menon, D. (2009). *Reinforced concrete design*, Tata McGraw-Hill Education, New Delhi, India.

Pradhan, B., and Bhattacharjee, B. (2009). "Performance evaluation of rebar in chloride contaminated concrete by corrosion rate." *Constr. Build. Mater.*, 23, 2346–2356.

Ranganathan, R. (1999). *Structural reliability, analysis and design*, Jaico Publication, Mumbai, India.

Stewart, M. G., and Rosowsky, D. V. (1998). "Time-dependent reliability of deteriorating reinforced concrete bridge decks." *Struct. Saf.*, 20, 91–109.

Tait, W. S. (1994). *An introduction to electrochemical corrosion testing for practicing engineers and scientists*, PairODocs Publications, Racine, WI.

Val, D. V., and Stewart, M. G. (2003). "Life-cycle cost analysis of reinforced concrete structures in marine environments." *Struct. Saf.*, 25, 343–362.

Vu, K. A. T., and Stewart, M. G. (2000). "Structural reliability of concrete bridges including improved chloride-induced corrosion models." *Struct. Saf.*, 22, 313–333.

Weyers, R. E. (1998). "Service life model for concrete structures in chloride laden environments." *ACI Mater. J.*, 95(4), 445–453.